

## Center-of-mass and breathing oscillations in small complex plasma disks

T. E. Sheridan\*

Department of Physics and Astronomy, Ohio Northern University, Ada, Ohio 45810, USA

(Received 11 March 2005; published 10 August 2005)

Center-of-mass and breathing oscillations of a complex (dusty) plasma disk are excited for  $n=3$  and 5 microspheres ( $\approx 10 \mu\text{m}$  diameter) with neutral argon pressures  $P \approx 1-4$  Pa. The mode frequencies and damping rates are determined directly from measured resonance curves. Millikan's coefficient for the Epstein drag force, the Debye length, and the particle charge is found by comparison with theory. The damping rates are the same for both modes and for  $n=3$  and 5, as predicted. Millikan's coefficient is found to be  $\delta=1.55 \pm 0.16$ , in agreement with  $\delta=1.44$  for diffuse reflection. A consistent value of the Debye length that decreases with pressure is measured. The average particle charge for  $n=3$  particles is found to be more negative than that for  $n=5$  particles for the same conditions, indicating that the effective ion collection area of the particles increases as their separation decreases.

DOI: 10.1103/PhysRevE.72.026405

PACS number(s): 52.27.Lw, 52.27.Gr, 52.35.Fp, 52.40.Kh

### I. INTRODUCTION

Microscopic dust particles can be levitated and confined in a plasma discharge. The dust particles form a system called complex, or dusty, plasma. Complex plasma is a system with unique physics that can be described with minimal reference to the normal plasma in which it is embedded. Monodisperse microspheres can be made to float in a horizontal monolayer where gravity and the electrostatic force on a particle balance, so that the complex plasma becomes effectively two dimensional. In the strong-coupling regime, the particles arrange themselves in a lattice that minimizes the total potential energy. If the radial confining potential has cylindrical symmetry, then the particles populate a circular disk. We refer to this system as a *complex plasma disk* [1].

The standard model of the complex plasma disk consists of  $n$  particles with identical mass  $m$  and charge  $q=-Ze$  moving in two dimensions [2-4]. The particles interact through a screened Coulomb potential [5,6] with a Debye length  $\lambda_D$  and are confined in a parabolic potential well [7] where the single-particle oscillation frequency is  $\omega_0$ . This model has been found to accurately describe the complex plasma disk in the strong-coupling regime. The quantities  $q$  and  $\lambda_D$  are difficult to measure directly and are often determined by comparing measured wave or normal modes with theoretical predictions.

A complex plasma disk of  $n$  particles has  $2n$  degrees of freedom and thereby  $2n$  normal modes. Most of these modes depend on the number and arrangement of the particles. However, there are three modes that exist for all complex plasma disks ( $n \geq 2$ ) [8]. These are the rotational, center-of-mass (c.m.), and breathing modes. The rotational mode has a frequency  $\omega=0$ , while the c.m. mode has a frequency  $\omega_0$  since the disk moves as a rigid body. The breathing mode has a frequency  $\omega_{br} \geq \sqrt{3}\omega_0$ , where  $\omega_{br} = \sqrt{3}\omega_0$  when the Debye length  $\lambda_D$  is infinite (i.e., for an unshielded Coulomb interaction) and  $\omega_{br}$  increases as  $\lambda_D$  decreases in a way that depends on both  $\lambda_D$  and  $n$  [1,3].

A number of experimental techniques have been developed to characterize the normal modes of a complex plasma disk. Modes have been excited using steplike excitations in "ringing" experiments [2], while the full mode spectrum has been studied by projecting the thermal motions of the particles onto the predicted normal modes [4]. In both experiments, agreement with the complex plasma disk model was quite good. More recently [9], the breathing mode of a complex plasma disk has been excited as a forced oscillation by modulating the plasma density, allowing a measurement of the breathing-mode resonance curve. A quadratic nonlinearity in the breathing mode was seen, and deterministic chaos has been observed [10].

In this paper, we demonstrate that modulating the plasma density can excite both the breathing and center-of-mass modes when the neutral pressure is low. This allows us to measure  $\omega_{br}$  and  $\omega_0$  as well as the damping rate for each mode. From theory [1,2], we know that  $\omega_{br}/\omega_0$  depends most sensitively on  $\lambda_D$  for small  $n$ . Experiments are reported for  $n=3$  and 5 particles. The damping rate is found to be the same for both modes and to increase linearly with pressure, allowing us to estimate Millikan's coefficient for the Epstein drag force [11]. The ratio  $\omega_{br}/\omega_0$  is used to determine the Debye length, which together with the interparticle spacing determines the particle charge  $q$ .

### II. THEORY OF THE COMPLEX PLASMA DISK

In the standard model of the complex plasma disk, it is assumed that all particles have identical charge  $q$  and mass  $m$ . The particles are confined by a parabolic potential well for which the single-particle oscillation frequency is  $\omega_0$ , and they interact through a screened Coulomb potential with a Debye length  $\lambda_D$ . The potential energy of the complex plasma disk is then [1-3]

$$U = \frac{1}{2} m \omega_0^2 \sum_{i=1}^n r_i^2 + \frac{q^2}{4\pi\epsilon_0} \sum_{\text{pairs}} \frac{\exp(-r_{ij}/\lambda_D)}{r_{ij}},$$

where  $r_i$  is the distance of the  $i$ th particle from the bottom of the well and  $r_{ij}$  is the separation between particles  $i$  and  $j$ . In

\*Electronic address: t-sheridan@onu.edu

the strong-coupling regime, the equilibrium positions of the particles are found by minimizing  $U$ . Using the dimensionless energy and length scales

$$U_0^3 = \frac{m\omega_0^2}{2} \left( \frac{q^2}{4\pi\epsilon_0} \right)^2, \quad r_0^3 = \frac{2}{m\omega_0^2} \frac{q^2}{4\pi\epsilon_0},$$

the total potential energy can be rewritten as

$$U = \sum_{i=1}^n r_i^2 + \sum_{\text{pairs}} \frac{\exp(-\kappa r_{ij})}{r_{ij}}, \quad (1)$$

where  $U$ ,  $r_i$ , and  $r_{ij}$  are now dimensionless quantities normalized by  $U_0$ ,  $r_0$ , and  $r_0$ , respectively. The Debye shielding parameter is

$$\kappa = \frac{r_0}{\lambda_D},$$

where  $\kappa=0$  corresponds to an unshielded Coulomb interaction.

In the center-of-mass mode, the complex plasma disk moves as a rigid body, so that the interparticle separation does not change. Consequently, the interparticle contribution to  $U$  is constant and the equation of motion is independent of  $n$ . For oscillations, say, in the  $x$  direction, the dimensionless equation of motion for the c.m. mode is

$$\ddot{x}_{c.m.} + 2\gamma\dot{x}_{c.m.} + x_{c.m.} = 0, \quad (2)$$

where the undamped oscillation frequency has the normalized value  $\omega_0=1$ . That is, the natural oscillation frequency for the c.m. mode is the single-particle oscillation frequency.

The dimensionless damping rate  $\gamma$  in Eq. (2) can be derived by assuming that the Epstein drag force is dominant [11]. For a spherical particle of radius  $a$  moving with a speed  $v$  in a neutral gas where the density is  $\rho_{gas}$  and the average molecular speed is  $\bar{c}$ , the drag force is

$$f = -\delta \frac{4}{3} \pi a^2 \rho_{gas} \bar{c} v,$$

where  $\delta$  is Millikan's coefficient. Here  $\delta=1$  for specular reflection and increases to  $\delta=1.44$  for diffuse reflection. For  $n$  particles, all moving in phase and with the same speed  $v$ , the total drag force is  $n$  times as great,

$$F = -n \left( \delta \frac{4}{3} \pi a^2 \rho_{gas} \bar{c} \right) v,$$

so that the dimensionless damping rate in Eq. (2) is

$$\gamma = \frac{1}{2m\omega_0} \left( \delta \frac{4}{3} \pi a^2 \rho_{gas} \bar{c} \right). \quad (3)$$

If the equilibrium particle positions and their motion in the breathing mode are known *a priori*, then the equation of motion for the breathing mode can be derived using Lagrangian mechanics [1]. This approach is most easily applied for systems with a small number of particles where the particles lie on the vertices of a regular  $n$ -gon (perhaps with a single particle at  $r=0$ ). For example, for three particles the equilibrium configuration is an equilateral triangle, while for

five particles the equilibrium configuration is a pentagon. In these cases, the particle motion in the breathing mode will be purely radial due to symmetry.

For three particles, each particle is a distance  $r$  from the center of mass (the bottom of the parabolic well) and the separation between particles is  $\sqrt{3}r$ . The potential energy in Eq. (1) is then

$$U_3(r; \kappa) = 3r^2 + \frac{3 \exp(-\sqrt{3}\kappa r)}{\sqrt{3}r}, \quad (4)$$

which depends only on  $r$  for a given value of  $\kappa$ . The equilibrium distance  $r_{eq}$  of each particle from  $r=0$  is found by minimizing  $U_3$  with respect for  $r$  for fixed  $\kappa$ ,

$$\left. \frac{dU_3}{dr} \right|_{r_{eq}} = 6r_{eq} - \frac{\exp(-\sqrt{3}\kappa r_{eq})}{r_{eq}} \left( 3\kappa + \frac{\sqrt{3}}{r_{eq}} \right) = 0.$$

The dimensional kinetic energy of the system is

$$T = \sum_{i=1}^n \frac{1}{2} m \dot{r}^2 = \frac{3}{2} m \dot{r}^2,$$

which using dimensionless variables becomes

$$T = 3\dot{r}^2.$$

Using the resulting Lagrangian, the *exact nonlinear* equation of motion for the breathing mode with  $n=3$  is

$$\ddot{r} + 2\gamma\dot{r} + r - \frac{1}{6} e^{-\sqrt{3}\kappa r} \left( \frac{3\kappa}{r} + \frac{\sqrt{3}}{r^2} \right) = 0. \quad (5)$$

The breathing frequency  $\omega_{br}$  (normalized by  $\omega_0$ ) can be found by linearizing Eq. (5) around  $r_{eq}$ . Alternatively,

$$\omega_{br}^2(\kappa) = \frac{1}{6} U_3''(r_{eq}; \kappa).$$

In Eq. (5) the damping rate  $\gamma$  is given by Eq. (3) since all particles move with the same speed.

The above analysis can also be applied to five particles in a pentagonal configuration, giving the potential energy as

$$U_5(r; \kappa) = 5r^2 + \frac{5e^{-\kappa d_1}}{d_1} + \frac{5e^{-\kappa d_2}}{d_2},$$

where the interparticle separation distances are

$$d_1 = r \sqrt{\frac{5-\sqrt{5}}{2}}, \quad d_2 = d_1 \frac{1+\sqrt{5}}{2}.$$

The normalized breathing frequency for  $n=5$  is then

$$\omega_{br}^2(\kappa) = \frac{1}{10} U_5''(r_{eq}; \kappa),$$

where  $r_{eq}$  is found by minimizing  $U_5$ . The damping rate  $\gamma$  for both the c.m. and breathing modes will again be given by Eq. (3).

Computed values of  $r_{eq}$  and  $\omega_{br}^2$  vs  $\kappa$  are shown in Fig. 1 for  $n=3$  and 5 particles. Here  $r_{eq}$  is greater for five particles, since the particles need to be farther from the bottom of the

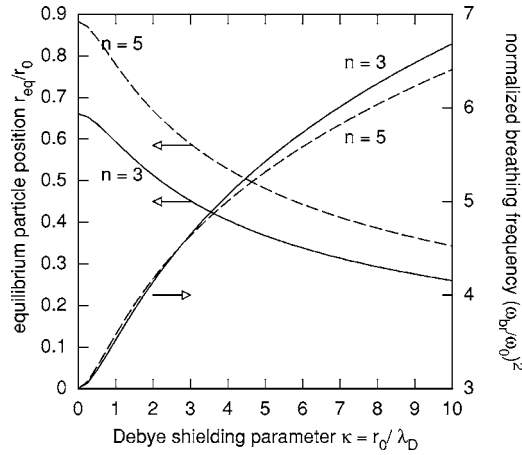


FIG. 1. Equilibrium particle position and squared breathing-mode frequency vs the Debye shielding parameter  $\kappa$  for  $n=3$  and 5 particles.

potential well to increase their separation. The value of  $r_{eq}$  decreases with  $\kappa$  since the repulsive force between particles decreases (for a fixed separation) as the Debye length decreases. The breathing frequency starts at the value  $\omega_{br}^2=3$  at  $\kappa=0$  (the unshielded Coulomb potential) and increases with  $\kappa$ . For  $\kappa \leq 4$  the predicted breathing frequencies for  $n=3$  and 5 are quite close together. For larger values of  $\kappa$  the breathing frequency for  $n=3$  increases more rapidly than that for  $n=5$ , as predicted by continuum theory [1] since the nearest-neighbor separation (on the unit circle) is greater for  $n=3$ .

### III. EXPERIMENTAL RESULTS

Experimental data were acquired in the dusty Ohio Northern University experiment (DONUT) [9], which is shown schematically in Fig. 2. The breathing and center-of-mass modes were excited as forced oscillations by amplitude-modulating (AM) the rf discharge power (13.56 MHz) at frequencies  $f=\omega/2\pi$  in the range  $\approx 1-5$  Hz. The c.m. mode is

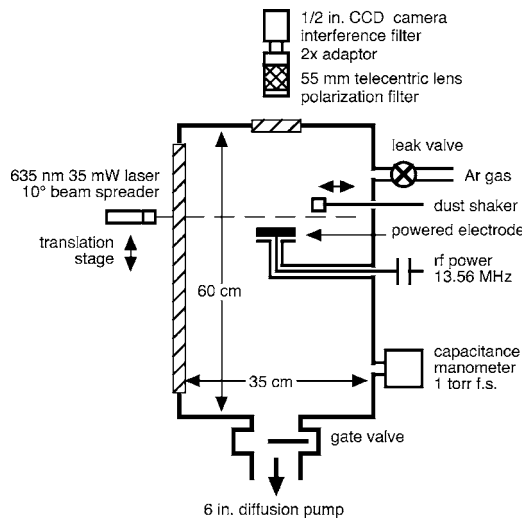


FIG. 2. Schematic of the dusty Ohio Northern University experiment (DONUT).

most easily excited at low pressures  $P \leq 4$  Pa. The forward rf power was  $\approx 3$  W. The impedance matching network between the rf amplifier and the plasma was unchanged during the experiments, and the rf power to the plasma varied slightly with pressure. The average dc bias on the electrode varied from  $-55$  V at the lowest pressure to  $-60$  V at the highest. In our experiment the confining potential is created using a ring with an inner radius of 25.5 mm and a depth of 1.9 mm placed on a 76-mm-diam electrode. Melamine formaldehyde resin microspheres with a nominal diameter of  $9.62 \pm 0.09 \mu\text{m}$ , as reported by the manufacturer (www.microparticles.de), were used.

Complex plasma disks with  $n=3$  and 5 particles were produced by introducing a large number of particles into the discharge. By slowly reducing the rf power, excess particles were then dropped to the electrode or lost radially. When the quantity of particles reached the desired number, the rf power was returned to its initial value. Experiments were performed with  $n=3$  particles for pressures  $P=0.87$  Pa (2.0% AM), 1.64 Pa (10.0% AM), and 3.13 Pa (10.0% AM) and for  $n=5$  particles at  $P=1.12$  Pa (5.0% AM), 1.43 Pa (5.0% AM), 1.96 Pa (5.0% AM), 2.45 Pa (10.0% AM), and 3.36 Pa (10.0% AM). Pressures were measured using a capacitance manometer (1 torr full scale). Two data sets were taken for  $n=5$  at 1.43 Pa and 2.45 Pa to gauge the repeatability of our results. In these cases the two measurements show excellent agreement, indicating that random errors are small.

Resonance curves were found by driving the system at a number of different frequencies while holding all other parameters constant. For each driving frequency, 30 frames of data were taken at 10, 15, or 30 frames per second depending on  $f$ . The set of particle positions  $\{x_i, y_i\}$  were measured in each frame (at a given driving frequency), and the center-of-mass coordinates  $x_{c.m.}$  and  $y_{c.m.}$  and disk radius  $R$  were computed using [9]

$$x_{c.m.} = \frac{1}{n} \sum_{i=1}^n x_i, \quad y_{c.m.} = \frac{1}{n} \sum_{i=1}^n y_i,$$

$$R^2 = \frac{2}{n} \sum_{i=1}^n [(x_i - x_{c.m.})^2 + (y_i - y_{c.m.})^2] = \frac{2}{n} \sum_{i=1}^n r_i^2. \quad (6)$$

(The use of  $\sum r_i/n$  by Melzer *et al.* [2] to characterize the breathing mode is incorrect for clusters with more than a single shell.) The quantities  $x_{c.m.}$ ,  $y_{c.m.}$ , and  $R$  were then fitted with a sinusoid at the driving frequency,

$$x_{c.m.} = x_0 + x_1 \sin(\omega t + \phi_x), \quad y_{c.m.} = y_0 + y_1 \sin(\omega t + \phi_y),$$

$$R = R_0 + R_1 \sin(\omega t + \phi_R), \quad (7)$$

from which the amplitude of the respective mode was determined. The total amplitude of the c.m. oscillation was computed as

$$r_{c.m.} = \sqrt{x_1^2 + y_1^2}.$$

The values of  $r_{c.m.}$  and  $R_1$  vs  $\omega$  were then fitted with the resonance curve for a driven, damped harmonic oscillator

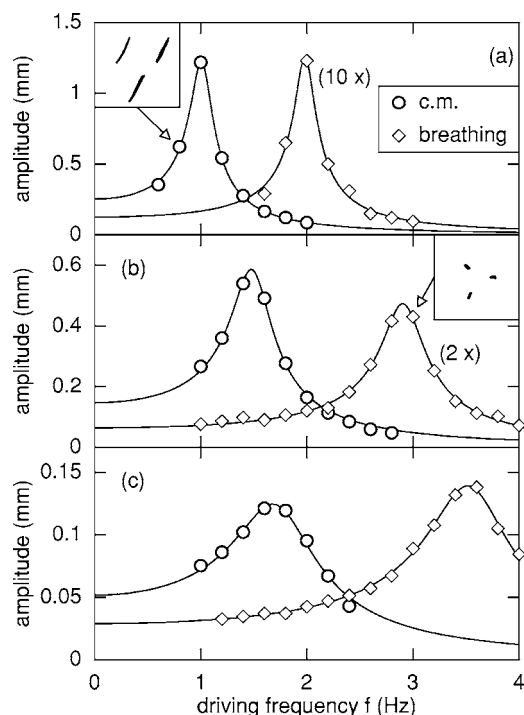


FIG. 3. Resonance curves for center-of-mass and breathing modes for  $n=3$  particles at pressures (a)  $P=0.87$  Pa, (b) 1.64 Pa, and (c) 3.13 Pa, with amplitude modulation of the rf power of 2.0%, 10.0%, and 10.0%, respectively. The insets ( $3.8 \text{ mm} \times 3.8 \text{ mm}$ ) display a top view of the cluster, showing c.m. motion at 0.87 Pa and 0.8 Hz and breathing motion at 1.64 Pa and 3.0 Hz.

$$A(\omega) = \frac{A_0}{\sqrt{(\omega^2 - \omega_0^2)^2 + 4\gamma^2\omega^2}},$$

allowing us to extract the maximum amplitude, natural frequency, and damping rate for each mode.

Resonance curves for experiments using  $n=3$  particles are shown in Fig. 3. These curves display the expected behavior. In all cases, well-defined resonances are seen for both the c.m. and breathing modes. The full width at half maximum (FWHM) of the resonance curves increases with pressure, indicating greater damping, while the natural frequencies shift upward as the pressure increases. The success of this analysis confirms that the two modes act as independent oscillators. A top view of the particle motion in each mode is shown in the insets. Note that the particle configuration closely approximates an equilateral triangle and that thermal motions are small compared to the normal mode motion.

#### A. Mode amplitude

The maximum amplitude of both modes decreases with increasing pressure. However, the amplitude of the c.m. mode appears to go to zero, while that of the breathing mode approaches a constant value. In our experiment, we find that c.m. oscillations are difficult to excite for  $P > 4$  Pa, while the breathing mode is easily seen for  $P \gtrsim 15$  Pa [9]. Since both modes have the same damping rate, this indicates that the force driving the c.m. mode goes to zero as the pressure increases (for constant rf power).

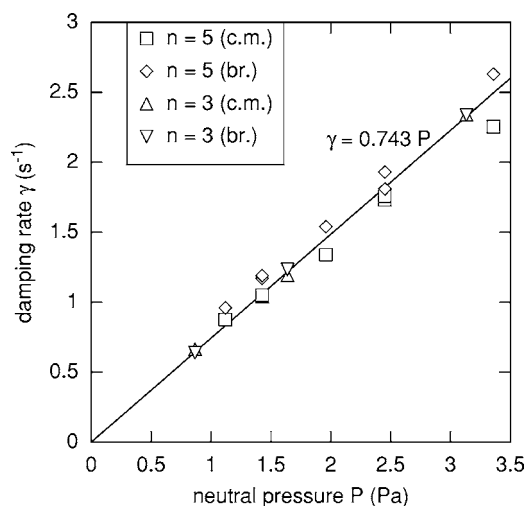


FIG. 4. Measured damping rates for center-of-mass and breathing modes with  $n=3$  and 5 particles as a function of neutral pressure.

Modulating the rf power produces a quasistatic modulation of the plasma density, which has the effect of varying the Debye length. For the breathing mode, this modulates the interparticle spacing, leading to a parametric resonance [12]. The c.m. mode is excited by a periodic motion of the potential well minimum. We can estimate the distance the minimum moves by referring to the low-frequency portions of the resonance curves in Fig. 3, since at low frequencies inertia is not important and the particles follow the potential well. At 0.87 Pa, the peak-to-peak displacement of the potential minimum is  $\approx 0.5$  mm, which is quite small. For these conditions, the particles are floating more than 10 mm above the electrode, so asymmetries in the electrode environment (e.g., the electrode support) may be responsible for the equipotential surfaces shifting horizontally to drive the c.m. mode.

#### B. Damping rate

The measured damping rates for  $n=3$  and 5 particles are shown in Fig. 4 as a function of neutral pressure. As expected, the damping rate increases linearly with pressure. The damping rates for  $n=3$  and 5 particles fall on the same line, indicating that the damping rate is the same for these two cases, as predicted. In both cases, the damping rates for the c.m. and breathing modes are very close, though for  $n=5$  the damping rate for the breathing mode is always slightly greater than the damping rate of the c.m. mode, which may indicate a small systematic error in the analysis. In particular, the motion of the center of mass becomes slightly elliptical (rather than linear) near the c.m. resonance.

A line passing through the origin has been fitted to all 20 data points, giving the relation

$$\gamma = (0.743 \pm 0.053)P,$$

where  $\gamma$  is in  $\text{s}^{-1}$ ,  $P$  is in Pa, and the uncertainty is twice the standard deviation of the slope. From theory [Eq. (3)] we predict that the *dimensional* damping rate should be

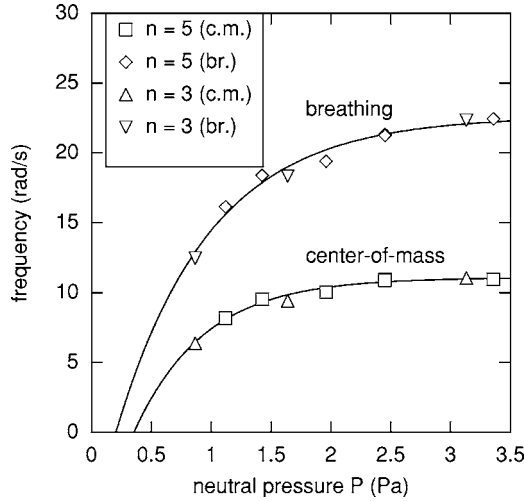


FIG. 5. Natural frequencies for breathing and center-of-mass modes with  $n=3$  and 5 particles.

$$\gamma = \delta \frac{4}{\pi \bar{c} a \rho_{\text{dust}}} P.$$

The manufacturer's reported particle diameter is  $2a = 9.62 \pm 0.09 \mu\text{m}$ . Interpolating from the electron microscope measurements of Liu *et al.* [11] (who used particles from the same manufacturer), the corrected particle diameter in our experiment is  $2a = 8.94 \pm 0.18 \mu\text{m}$ . Assuming an argon neutral temperature of 293 K ( $\bar{c} = 394 \text{ m/s}$ ) and the manufacturer's quoted density  $\rho_{\text{dust}} = 1.51 \text{ g/m}^3$ , we predict  $\gamma = \delta(0.479 \pm 0.016)P$ . The value of Millikan's coefficient required for agreement between experiment and theory is

$$\delta = 1.55 \pm 0.16.$$

This value is consistent with diffuse reflection,  $\delta = 1.44$ , as well as with the value measured by Liu *et al.* [11] in vertical resonance experiments ( $\delta = 1.44 \pm 0.19$ ). We conclude that the observed damping is due to the Epstein drag force.

### C. Natural frequency

The measured natural frequencies of the c.m. and breathing modes are shown in Fig. 5. For the same discharge conditions, the mode frequencies are effectively the same for  $n=3$  and 5. Since everything in the experiment was held constant except the pressure, we expect the c.m. frequency, which is determined by the confining potential well, should be independent of  $n$ , as verified in Fig. 5. The breathing frequency is also seen to be effectively independent of  $n$ . Theoretically (Fig. 1), we expect this to be the case if the Debye shielding parameter  $\kappa \leq 4$ . The uncertainty in the measured frequency due to random errors appears to be small since the repeated experiments at  $P=1.43$  and 2.45 Pa give nearly the same values of  $\omega_0$  and  $\omega_{br}$ .

The square of the normalized breathing frequency is shown in Fig. 6(a). The values of  $(\omega_{br}/\omega_0)^2$  fall over a narrow range from  $\approx 3.7$  to 4.2, for which  $\kappa \approx 1.5$ –2. For  $\kappa$  in this range, we predict that the breathing frequencies for  $n$

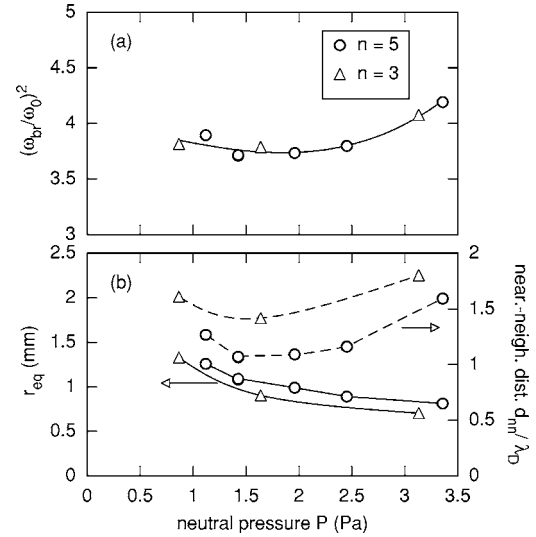


FIG. 6. (a) Squared, normalized breathing frequency vs pressure for  $n=3$  and 5 particles. (b) Equilibrium particle radius (solid lines) and nearest-neighbor separation  $d_{nm}$  (dashed lines) normalized by the Debye length  $\lambda_D$  vs pressure.

$n=3$  and 5 will be nearly the same, as confirmed by the data in Fig. 5. Experimentally, two effects are at work as the pressure increases. Initially, the c.m. frequency increases faster than the breathing frequency as the sheath edge moves closer to the electrode, so that  $(\omega_{br}/\omega_0)^2$  decreases. The value of  $(\omega_{br}/\omega_0)^2$  has a broad minimum around  $P \approx 2 \text{ Pa}$  and then increases with pressure, indicating that the Debye shielding parameter  $\kappa$  is increasing. For large pressures,  $\omega_0$  appears to be approaching a constant value as the pressure increases, while  $\omega_{br}$  continues to increase weakly, leading to a slow increase in  $(\omega_{br}/\omega_0)^2$ .

### D. Charge and Debye length

The charge and Debye length can be calculated from  $(\omega_{br}/\omega_0)^2$  [2] using the theory curves in Fig. 1. In particular, for a given  $n$ , the value of  $(\omega_{br}/\omega_0)^2$  determines the Debye shielding parameter  $\kappa$ . The equilibrium radii of the disks for  $n=3$  and 5 are

$$R_0 = \sqrt{2} r_{eq}.$$

That is, using the radius of the complex plasma disk computed from Eq. (6), the (dimensional) equilibrium radial distance of the particles from the bottom of the potential well can be found. This allows us to calculate  $r_0$  so that the Debye length  $\lambda_D$  and particle charge  $q$  can be calculated. The equilibrium distance of each particle from the bottom of the well  $r_{eq}$  is shown in Fig. 6(b). The equilibrium distance decreases with pressure, indicating that the particles are moving closer together, while for  $n=3$  the particles are closer to the bottom of the well than for  $n=5$  at the same pressure.

A plot of Debye length vs pressure is shown in Fig. 7 for  $n=3$  and 5 particles. For equivalent pressures, both experiments predict a consistent value of  $\lambda_D$  that decreases with pressure. Again, since the discharge conditions were the

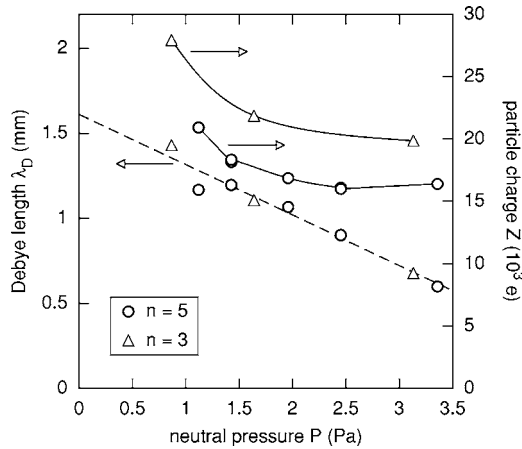


FIG. 7. Debye length  $\lambda_D$  and particle charge  $Z$  vs pressure for  $n=3$  and 5 particles.

same for both data sets, we expect that the Debye length should only depend on pressure and not on the number of particles. Assuming that the Debye length corresponds to the electron Debye length [6] and that the electron temperature  $T_e \approx 4$  eV, we calculate densities in the sheath of  $\approx 1-5 \times 10^8$  cm $^{-3}$ . These values are consistent with those expected for a low-pressure rf discharge, indicating that the transverse Debye shielding is indeed due to electrons. The decrease in Debye length with pressure is caused by two effects. First, for these conditions the plasma density increases approximately linearly with pressure. Second,  $T_e$  decreases weakly with increasing pressure. Both effects cause the Debye length to decrease as the pressure increases.

The dependence of the particle charge  $q = -Ze$  on pressure is also shown in Fig. 7. Here  $Z$  decreases as the pressure increases and is approximately constant for  $P \geq 2$  Pa. This effect is most likely due to a decrease in  $T_e$  with  $P$ . We clearly find that the particle charge for  $n=3$  is more negative than that for  $n=5$  for the same conditions. This is a real effect—we found consistent results for  $n=3$  and 5 for the damping rate, mode frequencies, and Debye length, in agreement with the model. Therefore, we expect that the model also provides a consistent estimate of the particle charge. A particle with a larger negative charge will have a more negative surface potential and, therefore, a smaller electron flux. Since the equilibrium charge is determined by the condition that the (average) electron and ion fluxes balance (neglecting secondary electron emission), a smaller electron flux implies a smaller ion flux. For  $n=3$  the particles are farther apart in Debye lengths than those for  $n=5$  [Fig. 6(b)], so we expect the  $n=3$  case to more closely approximate a single, isolated particle. That is, as the particle separation decreases the effective collecting area for ions increases.

#### IV. CONCLUSIONS

The center-of-mass and breathing modes of a complex plasma disk with  $n=3$  and 5 particles have been studied

theoretically and experimentally. A theory was developed that predicts (1) that the damping rates for both modes and for  $n=3$  and 5 particles should be the same at a given neutral pressure, (2) the dependence of the equilibrium particle displacement from  $r=0$ ,  $r_{eq}$ , on the Debye shielding parameter  $\kappa$ , and (3) the dependence of the ratio of the breathing frequency to the center-of-mass (c.m.) frequency on  $\kappa$ . This analysis does not require prior knowledge of any plasma parameters, unlike, for example, vertical resonance measurements which require the electric field gradient at the particle location.

We have shown that both the c.m. and breathing modes can be excited as steady-state oscillations by amplitude-modulating the rf power sustaining the discharge. Resonance curves for these modes were measured in DONUT as a function of neutral pressure for  $n=3$  and 5 monodisperse microspheres floating in a strongly coupled horizontal monolayer. The amplitude of each mode at a given driving frequency is recovered from a single history of the particle positions, indicating that the modes are effectively independent.

We have confirmed that the damping rate is the same for both modes and independent of  $n$  (for single-shell clusters) at a given pressure  $P$  and that the damping rate increases linearly with  $P$ . From the measured damping rates, we calculate that Millikan's coefficient for the Epstein drag force is  $\delta = 1.55 \pm 0.16$ . That is, the damping of the modes is well described by the Epstein drag force with diffuse reflection of atoms from the microspheres ( $\delta=1.44$ ).

We have shown that the center-of-mass frequency does not depend on  $n$  for  $n=3$  or 5. That is, the particles do not affect the shape of the confining potential well. In addition, we find that the breathing frequencies for  $n=3$  and 5 particles are quite close for our experimental conditions, as predicted for  $\kappa \lesssim 4$ .

The Debye shielding parameter  $\kappa$  was determined from the ratio of the breathing frequency to the c.m. frequency, and the equilibrium particle positions were measured directly, allowing us to calculate the Debye length and particle charge. We find a consistent value of the Debye length for  $n=3$  and 5 particles that decreases with pressure. That is, we have indirectly measured the Debye length in the sheath. The measured Debye length is consistent with electron Debye shielding. The charge on a particle for  $n=3$  is more negative than that for  $n=5$  for the same conditions. The reasons for this are unclear. However, this points out that the charge on a dust particle depends on the number of, and distance to, its neighbors. Consequently, the charge on a particle in a system may not be accurately determined by measuring or modeling an isolated particle.

#### ACKNOWLEDGMENT

I would like to thank K. D. Wells for assistance in acquiring and analyzing the data used in this paper.

- [1] T. E. Sheridan, *Phys. Plasmas* **11**, 5520 (2004).
- [2] A. Melzer, M. Klindworth, and A. Piel, *Phys. Rev. Lett.* **87**, 115002 (2001).
- [3] Minghui Kong, B. Partoens, and F. M. Peeters, *New J. Phys.* **5**, 23.1 (2003).
- [4] A. Melzer, *Phys. Rev. E* **67**, 016411 (2003).
- [5] U. Konopka, G. E. Morfill, and L. Ratke, *Phys. Rev. Lett.* **84**, 891 (2000).
- [6] M. Lampe, G. Joyce, and G. Ganguli, *Phys. Plasmas* **7**, 3851 (2000).
- [7] T. E. Sheridan, *J. Appl. Phys.* **98**, 023302 (2005).
- [8] B. Partoens and F. M. Peeters, *J. Phys.: Condens. Matter* **9**, 5383 (1997).
- [9] T. E. Sheridan, C. R. Buckley, D. J. Cox, R. J. Merrill, and W. L. Theisen, *Phys. Lett. A* **329**, 88 (2004).
- [10] T. E. Sheridan *Phys. Plasmas* **12**, 080701 (2005).
- [11] Bin Liu, J. Goree, V. Nosenko, and L. Boufendi *Phys. Plasmas* **10**, 9 (2003).
- [12] L. D. Landau and E. M. Lifshitz, *Mechanics*, 3rd ed. (Pergamon, Oxford, 1976), pp. 80–84.